# Community RNA-Seq: Multi-kingdom responses to living versus decaying root inputs in soil

Erin E. Nuccio[1]*, Nhu H. Nguyen[2], Ulisses Nunes da Rocha[3], Xavier Mayali[1], Jeremy Bougoure[4], Peter Weber[1], Eoin Brodie[5,6], Mary Firestone[5,6], Jennifer Pett-Ridge[1]*

[1]Physical and Life Sciences Directorate, Lawrence Livermore National Laboratory, Livermore, CA, USA; [2]Department of Tropical Plant and Soil Sciences, University of Hawai‘i at Mānoa, Honolulu, HI, USA; [3]Department of Environmental Microbiology, Helmholtz Centre for Environmental Research, Leipzig, Germany; [4]Centre for Microscopy, Characterisation & Analysis, The University of Western Australia, Perth, Australia; [5]Earth and Environmental Sciences, Lawrence Berkeley National Laboratory, Berkeley, CA, USA; [6]Department of Environmental Science, Policy and Management, University of California, Berkeley, CA, USA

Running header: Multi-kingdom responses to detrital root litter

*Corresponding authors: Erin Nuccio nuccio1@llnl.gov 925-423-9983, Jennifer Pett-Ridge pettridge2@llnl.gov 925-424-2882, Lawrence Livermore National Laboratory, Livermore CA, 94551 USA

## ABSTRACT

Roots are the primary source of organic carbon inputs to most soils. Decomposition is a multi-trophic process involving multiple kingdoms of microbial life, but typically microbial ecology studies focus on one or two major lineages in isolation. We used Illumina shotgun RNA sequencing to conduct PCR-independent SSU rRNA community analysis ("community RNA-Seq") to simultaneously study the bacteria, archaea, fungi, and microfauna surrounding both living and decomposing roots of the annual grass, *Avena fatua*. Plants were grown in $^{13}CO_2$-labeled microcosms amended with $^{15}N$-root litter. We identified rhizosphere substrate preferences for $^{13}C$-exudates versus $^{15}N$-litter using NanoSIMS microarray imaging (Chip-SIP). When litter was available, rhizosphere and bulk soil had significantly more Amoebozoa, which are potentially important yet often overlooked top-down drivers of detritusphere community dynamics and nutrient cycling. Bulk soil containing litter was depleted in Actinobacteria but had significantly more Bacteroidetes and Proteobacteria. While Actinobacteria were abundant in the rhizosphere, Chip-SIP showed Actinobacteria preferentially incorporated litter relative to root exudates, indicating this group's more prominent role in detritus elemental cycling in the rhizosphere. Our results emphasize that decomposition is a multi-trophic process involving cross-kingdom interactions, and the trajectory of carbon through this soil food web likely impacts the fate of carbon in soil.

## INTRODUCTION

Soil carbon is derived primarily from decomposed plant material (1, 2) and the fluxes that control the size of this pool are critical to the global carbon (C) cycle. The soil adjacent to plant roots (the rhizosphere) is a nexus for root C input, microbial C transformation, as well as C loss through decomposition (3, 4). Most root C is decomposed to $CO_2$, and the remainder typically undergoes multiple microbial transformations before it is stabilized. The spatial organization of soil habitats such as the rhizosphere and detritusphere (a region containing non-living organic matter) is particularly important for carbon and nutrient transfer by soil microbes and fauna, and the characteristics and rates of these microbial transformations determine how much carbon remains in soil (5). While it is widely recognized that fungi and soil fauna are instrumental to decomposition (6), less is known about how the greater soil food web of bacteria, archaea, fungi, and microfauna responds to decomposing litter in the rhizosphere and detritusphere.

To date, microbial ecology surveys studying litter decomposition using amplicon sequencing have primarily focused on bacteria or fungi, but decomposition is conducted by a broad array of organisms (7) including microfauna (here we use this umbrella term to include protists, nematodes and other soil invertebrates < 100 μm) (6, 8). Fungi play a key role in the decomposition of plant litter by providing the majority of the extracellular enzymes needed to depolymerize plant residues (9) and have been well-studied (10-13). Litter-associated microfauna may consume and directly break down litter (6), and protists and nematodes are also known to consume fungi and bacteria (8, 14-17); the presence of these consumers can affect both the microbial community composition and the rate of litter decomposition (18-24). Improving

61 our understanding of decomposition in soil necessarily requires us to consider the roles and
62 trophic interactions among the broader soil food web.
63
64 In the past decade, amplicon metabarcoding with high-throughput sequencing approaches have
65 allowed the identification of multiple groups of soil organisms in parallel (25-27). However,
66 PCR amplification has multiple layers of biases, including primer selection and bioinformatic
67 processing, and the lack of a universal primer set means multiple primer sets are required to
68 amplify taxonomically disparate groups (28-30). An alternative approach is to use amplification-
69 independent methods, such as shotgun RNA sequencing (RNA-Seq) for community analysis,
70 which we call "community RNA-Seq". This method not only reduces the inherent biases
71 associated with PCR (31-33), but since rRNA is an integral part of ribosomes that controls
72 protein synthesis across multiple kingdoms of life (34), direct sequencing of RNA allows us to
73 study active communities within Bacteria, Archaea, and Eukarya simultaneously without
74 amplification. Additionally, as most RNA is ribosomal RNA, the resulting sequences have
75 naturally high coverage of the ribosomal subunits most frequently used for taxonomic analysis
76 (e.g., 16S, 18S, 28S) (35), which allows greater sequencing depth of taxonomic markers than
77 metagenomic sequencing. To assess community composition, community RNA-Seq is followed
78 by either reassembling rRNA fragments into full ribosomal subunits or classifying the short
79 reads directly (35-38). Community RNA-Seq has been used to a limited degree in microbial
80 ecology due to the difficulty working with RNA in an environment such as soil, but initial
81 studies suggest it is a particularly useful approach to study protists in soil without PCR and
82 cultivation biases (35, 39). Eukaryotic primers are not universal for protists (40), which has led

to Amoebozoa being underrepresented in SSU rRNA gene surveys due to long SSU regions, and ciliates being overrepresented due to short SSU regions (39).

Methods that leverage isotopes as tracers of microbial activity (e.g. assimilation of substrates) are capable of adding another layer of ecological information to community analysis studies and have the potential to expand our understanding of food web dynamics and nutrient cycling in multi-trophic communities. Stable isotope probing (SIP) is a suite of powerful methods to study microbial ecophysiology in complex environments (41, 42) where a normally rare stable isotope (e.g., $^{13}C$, $^{15}N$, $^{18}O$) is added to the environmental matrix, and organisms that incorporate the labeled substrate become isotopically enriched over time in proportion to their activity (43, 44). Nucleic acid-SIP techniques (43, 45) are currently the most widely used means to directly connect microbial identity to substrate utilization. An iteration of nucleic acid-SIP is Chip-SIP where an imaging mass spectrometer (NanoSIMS) is used to determine the isotopic enrichment of rRNA hybridized to a phylogenetic microarray (46, 47). This method has a low $^{13}C$ enrichment requirement (0.5 atom%) relative to standard SIP, permits shorter isotope incubations, allows dual $^{13}C$ and $^{15}N$ labels in the same sample, and requires no amplification. Using this method, we can trace the fate of $^{13}CO_2$ after it is fixed by plants and released as $^{13}C$-rhizodeposits, and simultaneously trace detritus labeled with another isotope (e.g., $^{15}N$) to examine the relative incorporation of rhizosphere versus detritus in the same community.

In this work, we used shotgun RNA sequencing and Chip-SIP to study how living versus detrital root material alters the bacterial, archaeal, fungal, and microfaunal communities in the *Avena fatua* rhizosphere and surrounding bulk soil. We hypothesized that 1) the detritusphere would

106 increase saprotrophic fungi and eukaryotic grazers in the rhizosphere, and 2) rhizosphere
107 decomposers would consume both litter and root exudates, rather than specialize on either
108 resource alone.
109
110 **METHODS**
111 **Microcosm setup and soil collection**
112 Soils were collected at the Hopland Research and Extension Center (HREC, GPS 38.992982, -
113 123.067562) in Hopland, CA (USA), which experiences a Mediterranean climate (48). Soils are
114 a fine loam Alfisol complex (Ultic Haploxeralf mixed with a Mollic Palexeralf) with 1.7% C and
115 0.14% N (49). The top 10 cm of soil was collected from beneath a stand of naturalized *Avena*
116 *barbata* within a wild annual grassland community at 1 m intervals along a 10 m transect in
117 January. Large plant material was removed, including root pieces, and soil was sieved to 2 mm,
118 homogenized, then mixed with sand (1:1 w/w sand:dry weight soil) to improve drainage. The
119 mixed soil was packed into the main chamber of plastic microcosms (15 cm × 5 cm × 40 cm) to
120 a density of 1.2 g/cm$^3$ as previously described (Fig. 1a) (50, 51). *Avena fatua* seeds (Pacific Coast
121 Seed Inc., Tracy, CA, USA) were germinated in the dark for 7 days. One seedling per microcosm
122 was planted once the roots were greater than 1 cm long and after the shoot had emerged from the
123 seed. Plants were grown in a greenhouse under a 14-hour photoperiod and watered every 2-3
124 days to field water-holding capacity (approximately 50% saturation). After 6 weeks, the solid
125 divider separating the main chamber from the sidecar was replaced with a slotted divider (slots
126 ca. 10 cm x 4 mm) and the sidecar (5 mm deep) was filled with the experimental soil (Fig. 1a).
127

Sidecar experimental soil was freshly collected and sieved HREC soil (not mixed with sand), and half of the microcosms received $^{15}$N-labeled *A. fatua* root litter chopped to ca. 1 mm (78 atom % $^{15}$N; see Supplemental Methods for details regarding production of this material). The $^{15}$N isotopic tracer allowed us to use mass spectroscopy to detect the communities that were actively consuming litter-N. For the litter treatment (n=3), the soil was added to the sidecar in two layers, each approximately 2.5 mm deep: the bottom layer contained 75 g of soil with no litter, while the top layer contained the 75 g of soil amended with 0.4 g of $^{15}$N root litter. For the no-litter control (n=3), 150 g of soil was added to the sidecar. After packing the sidecars, microcosms were tilted at 45° to encourage root growth into the sidecars.

After filling the sidecar, plants were grown for 6 days in prior to $^{13}CO_2$ labeling, which is the amount of time it typically takes for roots to enter the sidecar. A 1.5m × 1.5m × 0.76 m plexiglass glovebox (Coy Laboratory Products, USA) was used as a labeling chamber at the UC Berkeley EPIC facility (49). The maximum chamber temperature was cycled between 26-28 ºC during the day and allowed to cool naturally to 20-22 ºC at night. Before dawn each day, the air in the chamber was cycled through a desiccator filled with soda lime to remove $CO_2$ until the chamber atmosphere reached < 25 ppm $CO_2$. The chamber was then filled with 99 atom % $^{13}CO_2$ until the concentration reached a set point of 400 ppm, and maintained at 400 ppm throughout the day using an SBA-5 model IRGA (PP Systems, 400 ppm $^{13}CO_2$ standard calibration) attached to a CR800 model datalogger (Campbell Scientific, Logan, UT, USA). Using this setup, the plants were labeled with $^{13}CO_2$ for 3 days.

After the 3 days of labeling, the front plates of the sidecars were removed to access an intact rhizosphere along the entire length of a root. Rhizosphere soil within 2 mm of the roots was excised using a scalpel. The soils were immediately placed in ice-cold Lifeguard RNA protectant solution (MoBio). Tubes were shaken for 2 minutes on a horizontal vortex adaptor (MoBio) on medium speed to release soil from the roots. The tubes were centrifuged at 2.5 × *g* for 1 min at 4°C, and any roots or floating root litter were removed with flame-sterilized forceps. The remaining soil was pelleted by centrifuging at 2.5 × *g* for 5 min at 4°C. After the supernatant was carefully removed, the pellets were immediately frozen on dry ice, and stored at -80°C for molecular analysis. Soil >4 mm from a root was treated as bulk soil. To collect bulk soils with litter, the top half of the sidecars that contained $^{15}N$ labeled litter was randomly excised using a scalpel. These samples often contained visible pieces of $^{15}N$ labeled roots. Bulk soil samples were processed in the same manner as rhizosphere soils. We collected a total of 12 soil samples: 2 locations (rhizosphere, bulk) × 2 litter conditions (litter, no litter) × 3 replicate microcosms. Hereafter, we refer to samples from the unamended control as “rhizosphere” and “bulk” and samples from the litter addition treatment as “rhizosphere-litter” and “bulk-litter”.

**RNA Extraction and Sequencing**

RNA was extracted in triplicate from 0.2 g soil per sample using the phenol-chloroform extraction protocol (52), modified from (53). Extracted nucleic acids were passed through the Allprep DNA/RNA Mini Kit (Qiagen Sciences, Maryland, USA) to separate RNA from DNA. RNA was treated with DNase using an on-column DNase digestion. For community RNA-Seq, metatranscriptomic libraries were prepared directly from total RNA without rRNA removal using the TruSeq RNA Kit (Illumina, Inc., San Diego, CA, USA) according to the

manufacturer's instructions. Metratranscriptomic libraries were sequenced on an Illumina GAIIX sequencer using 150 basepair (bp) paired-end sequencing at Lawrence Berkeley National Laboratory with an average of 9.5 million paired reads per sample.

**Sequence quality control and rRNA reconstruction**

Sequences were demultiplexed, and sequence quality was checked with FastQC (54). We used Trimmomatic (55) with default parameters with one exception; we removed the first 10 bp from the 5' end due to overrepresentation of this region in the dataset. Sequences shorter than 60 bp after trimming were removed. Reads that did not pair were discarded.

EMIRGE (36) was used to reconstruct near-full-length SSU rRNA sequences for Bacteria, Archaea, and Eukarya using the script "emirge_amplicon.py". The script was run on paired-end reads with the following parameters: mean insert length of 342, insert standard deviation of 100, and max read length of 151. The Greengenes 13_5 database clustered at 97% similarity was used to create the reference database for Bacteria and Archaea (56). The SILVA 114 NR database (57) was used to create the reference database for Eukarya. The database was also clustered at 97% as above. After the databases were created, the non-standard characters were altered as previously described (36). Bowtie indices required by EMIRGE were calculated for the databases using bowtie-build (58).

**OTU clustering and classification**

Bacterial and archaeal sequences were analyzed separately from eukaryotic sequences. Sequences were clustered using UPARSE (usearch_v7) (59) and analyzed using QIIME 1.8 (60)

196 at 97% sequence similarity. OTUs were classified using the RDP classifier (61), where bacterial
197 and archaeal classifications were trained using Greengenes 13_5 and eukaryotic sequences were
198 trained using SILVA 119NR (57). UCHIME (62) was selected to detect chimeras after testing
199 three chimera-checking tools (see Supplemental Methods). OTUs were required to be present in
200 at least two samples, and OTUs classified as chimeras or plant and algal chloroplasts were
201 removed from the dataset. In total, we analyzed 7229 unique full-length bacterial and archaeal
202 RNA sequences created by EMIRGE (1127 OTUs at the 97% similarity level), and 8488 unique
203 full-length eukaryotic RNA sequences created by EMIRGE (265 OTUs at 97% similarity level).
204
205 Since EMIRGE calculates a relative abundance estimate for each consensus sequence, a custom
206 OTU table (sample × OTU matrix) was created after OTU picking to incorporate relative
207 abundances of the consensus sequences into the microbial community analysis. To convert the
208 consensus sequence relative abundance into sequence abundance, we multiplied the total number
209 of reads that Bowtie mapped to the database by the relative abundance derived from the
210 "normalized priors", as per Miller, Handley (63): total mapped reads × consensus sequence
211 relative abundance = number of sequences per consensus sequence. Since each OTU can contain
212 multiple consensus sequences, we calculated the OTU sequence abundance by summing the
213 number of sequences for each consensus sequence within the OTU. The samples were then
214 rarefied to an even depth of 121 737 sequences for bacteria and archaea, and 27 668 sequences
215 for eukaryotes. As per the recommendations of Miller, Handley (63), OTUs with less than 0.01%
216 relative abundance were removed.
217
218 **Statistical Analysis**

Community differences were visualized by Principal Components Analysis (PCA) in QIIME using a pairwise weighted Unifrac distance matrix (64). To determine which OTUs differed in relative abundance between the litter and unamended treatments, we performed two sets of parametric t-tests in QIIME (group_significance.py): rhizosphere vs. rhizosphere-litter; bulk vs. bulk-litter. Only OTUs that were detected in all three replicates of at least one treatment were considered for analysis. P-values were corrected for multiple comparisons using an FDR correction. To calculate kingdom- or phylum-level relative abundances, relative abundances were summed for all OTUs within each group (kingdom for Eukarya, phyla for Bacteria and Archaea) and significant differences were determined using a t-test. Changes in the relative abundances for each group were determined by comparing litter-amended samples to their unamended control for bulk and rhizosphere soil separately (i.e., bulk vs. bulk-litter; rhizosphere vs. rhizosphere-litter).

**Chip-SIP Analysis**

To follow the movement of C and N from living plants and dead roots into the microbial community, we analyzed the rhizosphere of a microcosm containing both $^{15}N$ litter and $^{13}C$ exudates using Chip-SIP, a method that can detect and quantify $^{15}N/^{14}N$ and $^{13}C/^{12}C$ ratios of labeled RNA hybridized to microarrays (46, 47). Detailed methods for probe design, microarray synthesis and hybridization, NanoSIMS analysis, and data processing can be found in the Supplemental Methods. Briefly, we designed a microarray with probes using ARB (65) for the 180 most abundant Bacteria, Archaea, and Eukarya (fungi, protists, nematodes) OTUs found in this study, as well as probes targeting plant chloroplasts; a taxonomy summary of the probes used in this study is available in Table S1. Ten distinct probes per OTU were printed in three

242 replicate blocks on the microarray. We produced 2 microarrays for this sample, one to detect
243 RNA binding, and a second to detect RNA $^{13}C$ and $^{15}N$ isotopic enrichment with NanoSIMS. To
244 detect RNA binding, RNA was labeled with Alexafluor 532 dye using the Ulysis kit (Invitrogen),
245 fragmented with fragmentation buffer (Affymetrix), purified, concentrated and hybridized onto
246 the first array. For NanoSIMS analysis, unlabeled RNA was again fragmented, purified and
247 concentrated and then hybridized to the second array. The array with fluorescently labeled RNA
248 was imaged with a Genepix 4000B fluorescence scanner. The second array (with non-
249 fluorescently labeled RNA) was also imaged with the fluorescence scanner to allow navigation
250 to analysis spots in the NanoSIMS. Data were collected on the LLNL NanoSIMS 50 in pulse
251 counting mode using aperture slit 3 and entrance slit 5, first collecting $^{12}C^{14}N^-$ and $^{12}C^{15}N^-$, and
252 then $^{12}C^{14}N^-$ and $^{13}C^{14}N^-$. The resulting data were visualized as a stitched isotope map (Fig. S1)
253 and data extracted as per Mayali, Weber (46).
254
255 The proportion of isotopes is presented as a relative atom percent excess (APE) enrichment ratio
256 of $^{13}C$ to $^{15}N$ ($^{13}C$-APE:$^{15}N$-APE) to indicate substrate preferences, where lower values indicate
257 greater $^{15}N$ enrichment in the RNA, and higher values indicate greater $^{13}C$ enrichment in the
258 RNA. Due to the higher background of $^{13}C$ compared to $^{15}N$ on the array, we used a
259 normalization factor of 1.7 to calculate these relative enrichment ratios, as previously described
260 (66). Higher relative enrichment in $^{15}N$ is interpreted as having a preference for amended $^{15}N$
261 root litter whereas higher relative enrichment in $^{13}C$ is interpreted as having a preference for $^{13}C$
262 root exudates. We note that this is a relative measure as the $^{13}C$ values do not reflect the total $^{13}C$
263 ingested, as part of the $^{13}C$ consumed is lost through respiration (66).
264

## RESULTS

### *Community Structure from Reconstructed SSU rRNA*

The addition of root litter and the presence of living roots both significantly altered the bacterial and eukaryotic communities relative to bulk soil; both the bacterial and eukaryotic communities had significantly different clusters per treatment by PERMANOVA analysis (Fig. 2) (see Table S2 for F Tables), though the eukaryotic communities had more overlap (Fig. 2b). The bulk-litter communities were the most distinct group in ordination space for both bacteria and eukaryotes. Root litter had the strongest effect on both the bacterial and eukaryotic communities, explaining 30% and 28% of the variance in those communities, respectively (2-way PERMANOVA: bacteria $F_{1,4} = 7.2$, $r^2 = 0.30$, $p > 0.001$; eukaryotes $F_{1,4} = 5.4$, $r^2 = 0.28$, $p > 0.001$). The presence of a living root also significantly altered these communities, which was strongly significant for bacteria (2-way PERMANOVA: $F_{1,4}= 4.7$, $r^2 = 0.20$, $p = 0.006$), and was slight but significant for eukaryotes (2-way PERMANOVA: $F_{1,4} = 3.2$, $r^2 = 0.17$, $p = 0.029$).

### *Phylum and Kingdom Level Responses*

We observed broad patterns in relative abundance of bacteria and eukaryotes at the phylum and kingdom level, respectively. Proteobacteria and Actinobacteria were the most abundant bacterial groups in the rhizosphere (Fig. 3a). Actinobacteria, Acidobacteria, and Chloroflexi were significantly reduced in the bulk-litter treatment (t-test: $p < 0.05$) (Fig. 3a), while Bacteroides and Proteobacteria were significantly more abundant in the bulk-litter treatment. For the eukaryotes, Amoebozoa were significantly more abundant in presence of litter in both rhizosphere and bulk soils compared to their respective unamended controls (Fig. 3b). In unamended bulk soil, Rhizaria were significantly more abundant. While the litter-containing

288 treatments appear to have less Fungi, these differences were not significant ($p > 0.5$) compared to
289 the unamended controls.
290
291 ***Significant Litter and Rhizosphere Responders***
292 We compared litter-amended soil to the unamended control for bulk soil and the rhizosphere
293 (Fig. 4). In bulk soil, litter additions significantly increased specific groups of protists, fungi, and
294 bacteria, whereas litter amendments in the rhizosphere had fewer significant responders. Protists
295 from multiple lineages were more abundant in the presence of litter (Fig. 4b), where *Colpoda* sp.
296 (Alveolata), *Glaseria* sp. (Amoebozoa), and *Naegleria* sp. (Heterolobosea) were some of the
297 most abundant genera (Fig. 4b). Platyophyra sp. (Alveolata) were abundant in the rhizosphere
298 and bulk soil when litter was present. Fungal saprotrophic *Chaetomium* sp. (Ascomycota)
299 responded the most strongly to litter, while the other fungal taxa were more abundant in the
300 absence of litter (*Cryptococcus* sp., *Davidiella* sp.). The bacterial taxa that strongly responded to
301 the litter were *Massilia* sp. in the Oxalobacteriaceae (Proteobacteria), and OTUs in the families
302 Paenibacilliaceae (Firmicutes), and Sphingobacteriaceae (Bacteroidetes) (Fig. 4a). When the
303 rhizosphere was amended with litter, only bacteria in the family Sphingobacteriaceae
304 (Bacteroidetes) significantly increased. Detailed taxonomic results can be found in Table S3.
305
306 When no litter was present, an unclassified fungus in the phylum Basidiomycota and
307 *Platyophrya* sp. (Alveolata) responded strongly to the rhizosphere. Protists from the Rhizaria,
308 (phylum Cercozoa) were more abundant in unamended soil, particularly unclassified genera
309 within the classes Thicofilosea and Eugliphida. Taxa that were more prominent in unamended

310 bulk soil were from the Rhodospirillaceae (Proteobacteria), Bacillaceae (Firmicutes),
311 Solirubrobacterales (Actinobacteria).
312
313 ***Chip-SIP: Substrate Preferences***
314 We used Chip-SIP stable isotope analysis to distinguish substrate preferences in bacterial,
315 archaeal, and eukaryal taxa between root exudates ($^{13}C$ enriched) and decaying root litter ($^{15}N$
316 enriched). In the $^{13}C$-labeled rhizosphere sample amended with $^{15}N$-litter, we detected 42
317 isotopically enriched OTUs with Chip-SIP (Fig. 5; 1 archaea, 33 bacteria, 8 fungi); protists
318 probes were on the array but were not enriched during this 3-day $^{13}CO_2$ experiment (see probe
319 taxonomy in Table S1). No microorganism's RNA was enriched solely in $^{13}C$ or $^{15}N$, and only
320 the plant probes on the array were solely enriched with $^{13}C$ and had the highest relative
321 enrichment ratios of the dataset (Table S4). As a phylum, the Actinobacteria OTUs contained a
322 relatively higher proportion of $^{15}N$ than $^{13}C$: 6 of 7 enriched taxa fell on the lower range of the
323 $^{13}C/^{15}N$ spectrum (0.2 – 0.8). Xanthobacteriaceae bacteria, *Sphingomonas* bacteria, and
324 Eurotiomycetes fungi were also more enriched in $^{15}N$ relative to the other Chip-SIP taxa (Table
325 S4), however RNA of *Sphingomonas* sp. and Eurotiomycetes were also equally or more enriched
326 in $^{13}C$, suggesting that these organisms consumed both fresh and detrital plant material during
327 this 3-day study. Organisms with preference for rhizosphere exudates were 2 *Bacillus* OTUs, 2
328 Rhizobiales OTUs (Bradyrhizobiaceae, *Rhizobium*), and 2 Burkholderiales OTUs (*Massilia*).
329 Fungi from the Ascomycota (Dothideomycetes, Eurotiomycetes, Leotiomycetes) and
330 Basidiomycota (Agaricomycetes) tended to be equally or slightly more relatively enriched in $^{13}C$
331 than $^{15}N$.
332

## DISCUSSION

While it is widely recognized that fungi and soil fauna are instrumental to decomposition (6), less is known about how decomposition processes interact with the greater soil food web, which includes bacteria, archaea, fungi, and microfauna. To this end, we directly sequenced total RNA to identify bacteria, archaea, and eukaryotes in the presence and absence of root litter, and determined how the presence of a living root altered these communities. We also used NanoSIMS-enabled microarray analysis (Chip-SIP) to track the fate of $^{15}N$ root litter and $^{13}C$ rhizodeposits and identified the substrate preferences of abundant organisms in the rhizosphere amended with litter.

### *Protists were abundant in decomposing litter and are important for nutrient cycling*

We found that protists were abundant in decomposing litter in the presence and absence of living roots. In soil, decomposition is carried out by bacteria, fungi, mesofauna (e.g. microinvertebrates), and macrofauna (e.g. earthworms, millipedes), whose shredding action create smaller particles that are more readily accessible to microbes (6). On the other hand, soil microfauna (e.g. protists, nematodes) primarily consume bacteria and fungi (67-69). Those that feed directly on soil bacteria and fungi are thought to indirectly influence the decomposition of soil organic matter in multiple ways. For example, not only can microfauna alter the composition of bacterial and fungal decomposers, they can also accelerate the turnover of microbial biomass and excrete nutrients derived from microphagy (12, 70), which in turn can enhance litter decomposition (24). Protists can stimulate microbial nutrient cycling through the microbial loop (71, 72), which is a phenomenon where N contained in microbial biomass is higher than the N demand of protists, and predation ultimately leads to an increase in available N after excretion.

356 The high abundance of protists we observed in decomposing litter may have altered the flow of
357 nutrients though grazing and is an important dynamic currently missed in many bacterial and
358 fungal litter decomposition studies.
359
360 ***Amoebas are potentially important yet overlooked top-down driver of detritusphere community***
361 ***dynamics and nutrient cycling***
362 Rhizaria (Cercozoa), Amoebozoa, and Alveolata were the most abundant protists in our soils. A
363 previous metatranscriptomic study also found that Rhizaria and Amoebozoa were abundant in
364 grassland soils relative to peatlands (39). Interestingly, we predominantly observed Rhizaria in
365 unamended bulk soil, whereas Amoebozoa were more abundant when litter was present in both
366 bulk soil and the rhizosphere. This suggests these two abundant groups inhabit different niches
367 within the soil environment. In a complementary transcriptomics dataset from this soil (52),
368 Amoebozoa expression of exoproteases was highest in the litter-containing rhizosphere and bulk
369 soils (Figure S2), which further suggest these organisms play an active role in microbial
370 community dynamics in the detritusphere. Microfaunal predation is generally overlooked as a
371 top-down driver of microbial community assembly (73). Amoebas in particular are known to be
372 mycophagous or bacterivores (15, 16) and can influence microbial community structure (12). As
373 the Amoebozoa Supergroup is typically missed in amplicon analysis (74), our results suggest
374 Amoebas may be an overlooked contributor to microbial community dynamics and nutrient
375 cycling in the detritusphere.
376
377 ***Rhizosphere and bulk soil harbor unique litter-decomposing communities***

Each treatment in this study had a unique microbial community, where the rhizosphere and bulk soil contained distinct assemblages of potential decomposers. In particular, the bulk-litter community had significantly more Bacteroidetes, Proteobacteria (Oxalobacteriaceae, Caulobacteraceae, Bacteriovoraceae), and saprotrophic *Chaetomium* fungi relative to the unamended control, but was depleted in Actinobacteria and Acidobacteria. In the rhizosphere, both sequencing and $^{15}$N-litter Chip-SIP identified members of the Sphingobacteriaceae as responders to litter; Chip-SIP also identified Xanthobacteriaceae bacteria and Eurotiomycetes fungi as consumers of $^{15}$N-litter in the rhizosphere. Previous stable isotope probing studies have identified taxa from the Actinobacteria, Firmicutes, and Bacteroidetes as bacterial decomposers of plant material in soil (75, 76), and taxa from the Burkholderiales, Caulobacteriales, Rhizobiales, Sphingobacteriales and Xanthomonadales as cellulose-degrading bacteria (77). The low abundance of Actinobacteria in the bulk-litter soil was unexpected given that they are commonly identified as soil decomposers (75-77), and the trend toward reduced total fungi transcripts (Fig. 4b) did not support our initial hypothesis. In bulk-litter soil, a different suite of decomposers may have preferred the root litter in our system (e.g., Bacteroidetes, *Chaetomium* fungi) instead of Actinobacteria. Alternatively, the reduction in Actinobacteria and trend toward reduced total fungi in the presence of litter might be explained by interactions among soil microbes. As Amoebozoa and bacterial predators (e.g., Bacteriovoraceae) were abundant in the litter-containing treatments, it is possible that the low abundance of common decomposers in the presence of litter might have been driven by fungal or bacterial grazing (78, 79). Members of the Oxalobacteriaceae have also been shown to consume fungi (80), though we did not identify any known mycophageous genera in our dataset. We also note that we did not observe any macrofauna or mesofauna sequences in the dataset; macrofauna (and possibly mesofauna) would

401 have been removed during the processing phase of soils, or because the amount of soil extracted
402 for DNA was too small in volume.
403
404 ***Isotopic tracers identify substrate preferences in the rhizosphere***
405 The Chip-SIP results helped us to start to disentangle microbial substrate preferences in the
406 rhizosphere. We used two isotopic tracers to determine if soil microbes preferentially consumed
407 $^{13}$C-exudates or $^{15}$N-litter. In the rhizosphere-litter treatment, the Actinobacteria tended to prefer
408 $^{15}$N-litter, while Fungi and the Rhizobiales tended to assimilate $^{15}$N-litter and $^{13}$C-exudates
409 equally, with a slight preference for $^{13}$C-exudates. While Actinobacteria were the second-most
410 abundant phylum in the rhizosphere treatments, the Chip-SIP data indicated that they may have
411 preferred to consume detrital SOM in this habitat; this is consistent with recent findings where
412 the Actinobacteria had the highest CAZyme gene expression in the detritusphere or aging
413 rhizosphere (rhizosphere >20 days old) (52). Actinobacteria have been identified as plant- or
414 cellulose-degraders by density gradient SIP (75-77). This highlights that 16S patterns alone have
415 a limited ability to determine substrate preferences and require additional information to assess
416 microbial ecophysiology, such as through isotope tracing or activity-based analyses.
417
418 ***Relevance of the microbial food web for soil C cycling***
419 The multi-trophic changes we observed in our study are relevant for soil carbon cycling.
420 Microbial communities have diverse arrays of physiological strategies for consuming carbon
421 substrates (7). Changes in the microbial community can influence the rate of decomposition and
422 decomposition products (7, 81), and are expected to alter the diversity of compounds available
423 for sorption to mineral surfaces (82). For example, we found that Actinobacteria decreased in the

424 bulk-litter treatment while *Chaetomium* fungi increased, which likely altered the composition of
425 exoenzymes available to breakdown plant material and can further influence the rates and types
426 of organic matter that can be degraded (83, 84). Microbial bodies themselves define the forms of
427 C available for stabilization, such as cell wall components, polysaccharides, enzymes,
428 intracellular sugars, and intermediate products of litter decomposition (7, 83, 85-87); these
429 components can have different residence times in soil (83, 88). Selective predation, such as by
430 protists or Bacteriovoraceae, can alter the both the taxonomic and functional composition of the
431 soil microbiome (73). In addition, predation by protists potentially diversifies and alters forms of
432 C available for sorption to mineral surfaces since the microbial polymers undergo digestion
433 before excretion, and protists have been shown to selectively retain particular classes of
434 metabolites (89). Thus, the trajectory of carbon through the soil food web likely impacts the fate
435 and persistence of carbon in soil.
436

437 **CONCLUSIONS**

438 Using metatranscriptomic sequencing of total RNA, we identified the bacterial, archaeal, and
439 eukaryotic communities that responded to detrital root litter in rhizosphere and bulk soil. Litter-
440 decomposing communities differed depending on the presence and absence of a root, where the
441 litter-amended bulk soil had the most distinct microbial and protist communities. The litter-
442 amended rhizosphere and bulk soil contained significantly more Amoebozoa than the
443 unamended controls, and grazing by these protists may be an important top-down control on the
444 microbial community during litter decomposition and alter the trajectory of carbon through the
445 soil food web. Chip-SIP NanoSIMS analysis identified substrate preferences for $^{15}N$ root detritus
446 or $^{13}C$ rhizodeposits fresh root exudates and gave insights into food web processes that were not

447 discernible from compositional analyses alone. Future work combining shotgun RNA
448 community analyses and stable isotopes has the potential to improve our ability to track nutrients
449 through multi-trophic food webs.
450

451 **ACKNOWLEDGEMENTS**

452 This research was supported by the U.S. Department of Energy Office of Science, Office of
453 Biological and Environmental Research Genomic Science program under awards SCW1421,
454 SCW1589, and SCW1678 to JPR and under awards DE-SC0010570, DOE-SC0016247, and DE-
455 SC0020163 to MKF. Work conducted at Lawrence Livermore National Laboratory was
456 supported under the auspices of the U.S. DOE under Contract DE-AC52-07NA27344. Work
457 conducted at Lawrence Berkeley National Laboratory was supported under Contract DE-AC02-
458 05CH11231. We thank Katerina Estera Molina and Shengjing Shi for laboratory assistance,
459 Donald Herman for assistance with the EPIC $^{13}CO_2$ labeling system, Ulas Karaoz for data
460 management assistance, and Ella Sieradzki for the Acanthamoebidae supplemental figure.
461

462 **CONFLICTS OF INTEREST**

463 The authors declare no conflicts of interest.
464

## FIGURES

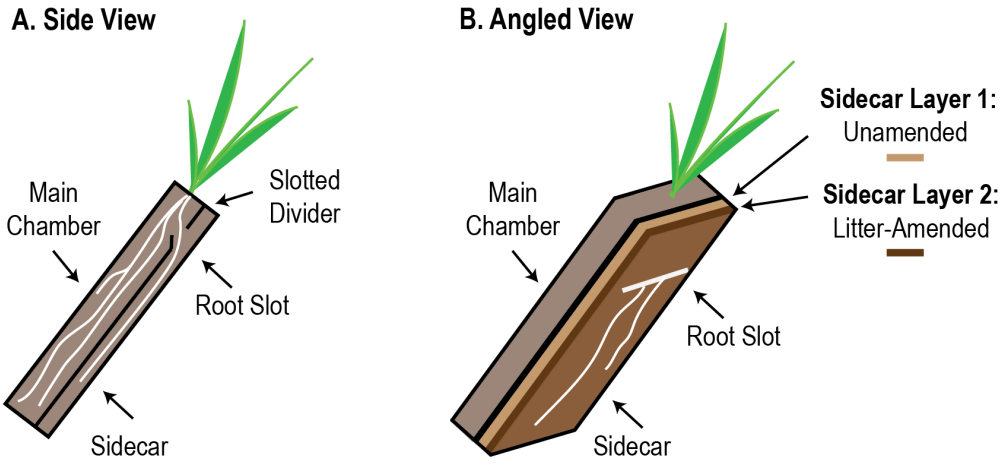


**Figure 1:** Microcosm design and sampling strategy. (A) Microcosms had a main chamber that housed the plant during plant growth and maturation. The main chamber was separated from an auxiliary root chamber (the sidecar) by a solid divider; microcosms were tilted to promote the growth of roots. After 6 weeks, the solid divider was removed and replaced with a slotted divider to permit root growth into the sidecar, and the sidecar was then filled with the experimental soil. (B) Half of the experimental soils were amended with $^{15}N$-labeled root detritus (layer 2), which was placed on top of unamended soil (layer 1). Unamended controls were prepared in the same manner, but no litter was added to the second layer. After 6, days the roots entered the sidecar, and the plants were then pulse labeled for 3 days with $^{13}CO_2$ and harvested. Roots grew along the face of the sidecar and rhizosphere soil (<2 mm from root) and bulk soil (>4 mm from root) were excised with a scalpel.

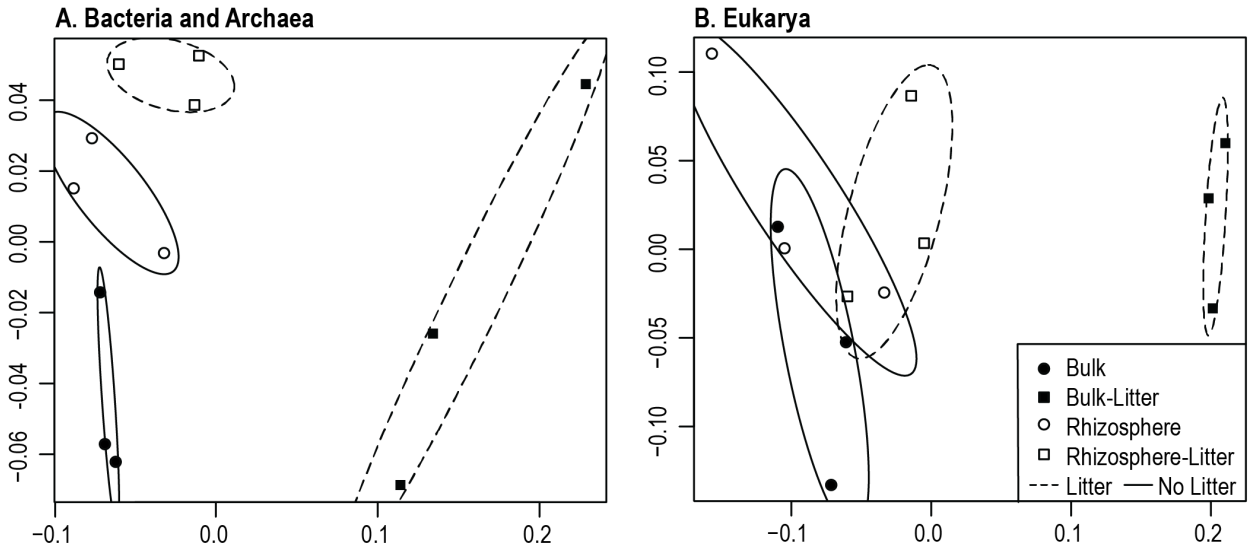


480

481 **Figure 2:** Community RNA-Seq non-metric multidimensional scaling ordinations for (A)
482 Bacteria and Archaea (assembled 16S rRNA), and (B) Eukarya (assembled 18S rRNA) in the
483 *Avena fatua* rhizosphere and bulk soil in response to litter amendments. Soil was sampled after 3
484 days of fresh root growth into the microcosm sidecars. Filled symbols represent bulk soil, while
485 hollow symbols represent rhizosphere soil. Squares indicate litter addition while circles had no
486 litter added. Ovals represent the 95% standard error of the weighted average of scores per group
487 (r package: ordiellipse) for litter treatments (dashed lines) and no litter (solid lines).

488

489

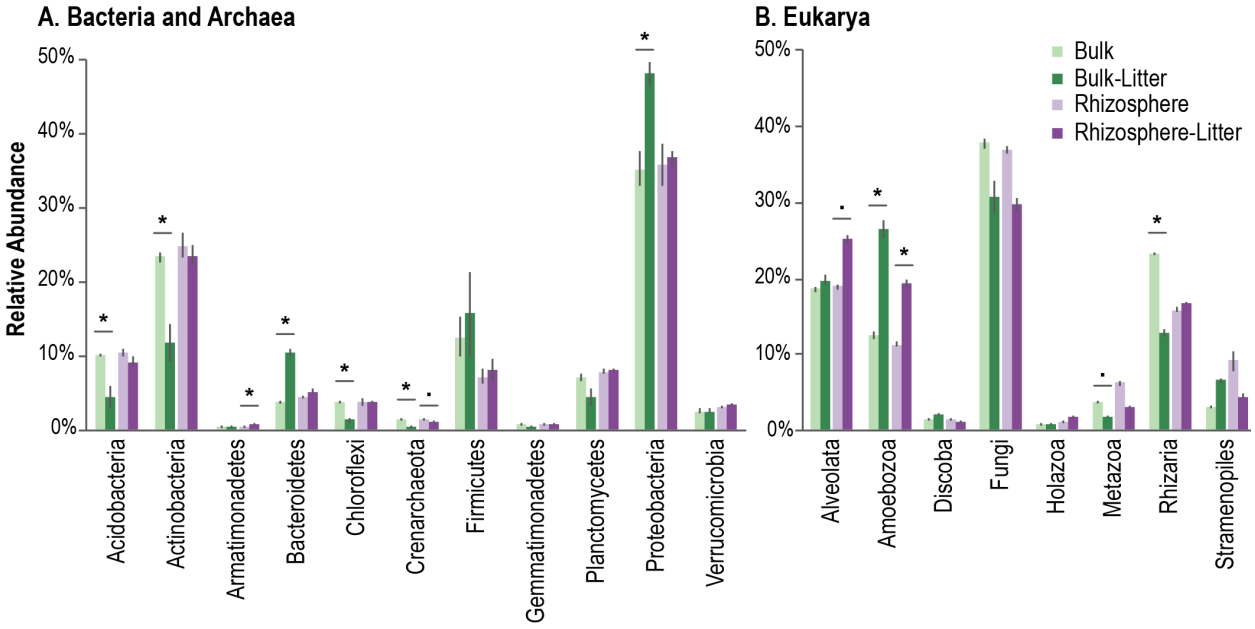


490

491 **Figure 3:** SSU rRNA relative abundance at the (A) phyla level for Bacteria and Archaea, and
492 (B) kingdom for Eukarya. The treatments were as follows: bulk soil with no litter amendment
493 (bulk, light green) and amended with root litter (bulk-litter, dark green), and rhizosphere soil
494 with no litter amendment (rhizosphere, light purple) and amended with root litter (rhizosphere-
495 litter, dark purple). Groups that significantly differed in relative abundance with litter
496 amendments are indicated by * (t-test: $p < 0.05$) (Bulk vs. Bulk-Litter; Rhizosphere vs.
497 Rhizosphere-Litter), and "." indicates marginal significance ($p < 0.1$).

498

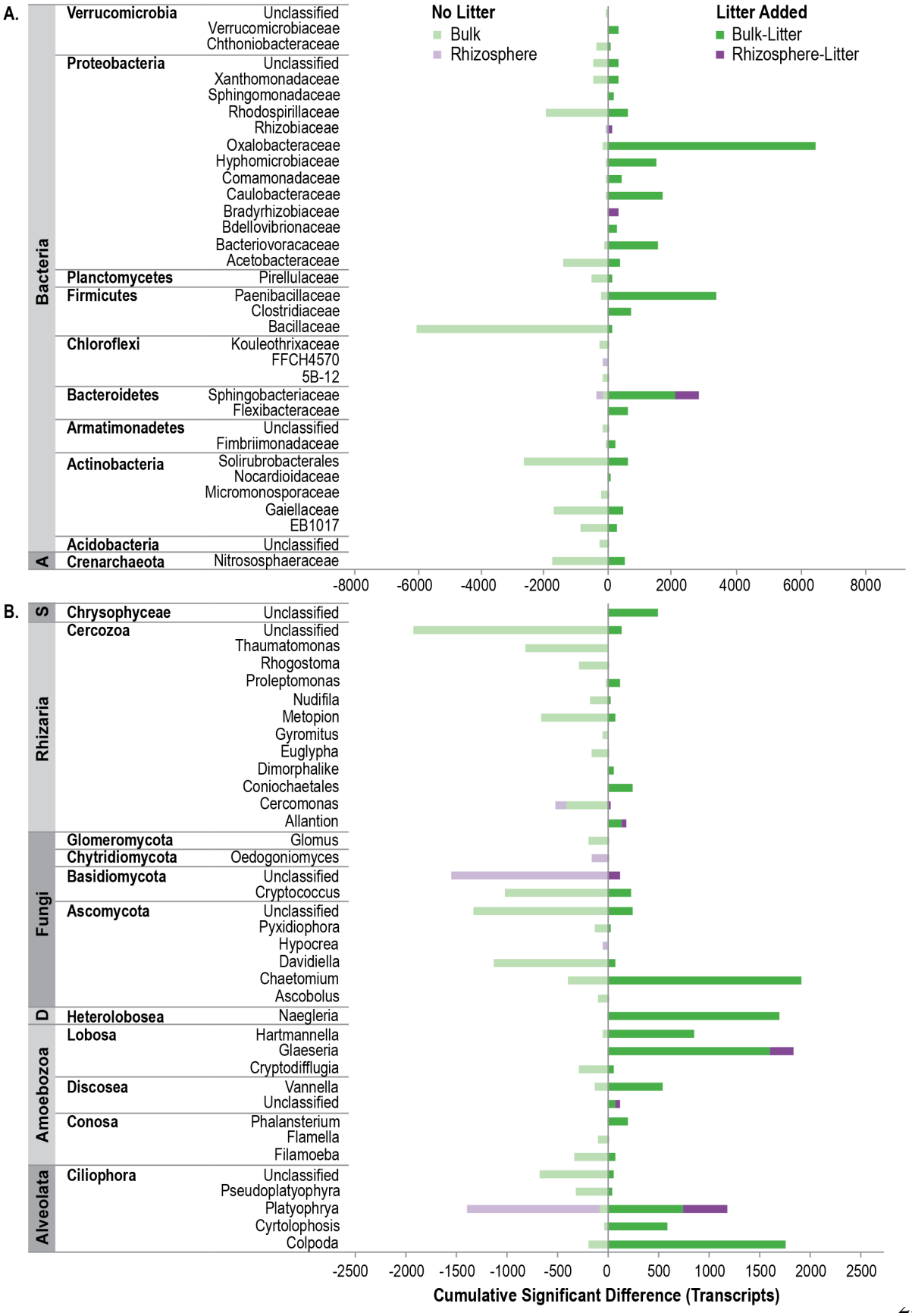

500 **Figure 4:** Cumulative significantly-different transcripts for positive and negative responders to
501 detrital root litter in bulk soil and the rhizosphere. The effects of litter amendments were
502 calculated separately for bulk soil and rhizosphere soil, where “dark green” indicates cumulative
503 positive responses to litter for bulk soil, and “dark purple” indicates cumulative positive
504 responses to litter for rhizosphere soil. Negative responses to litter (or preference for unamended
505 soil) are “light green” for bulk soil and “light purple” for rhizosphere soil. Transcripts were
506 aggregated by taxonomic family for Bacteria and Archaea and genus for Eukarya; OTU
507 transcript abundances were averaged across replicates (n=3) prior to aggregation. Multiple
508 comparisons were accounted for using a FDR p-value correction.
509

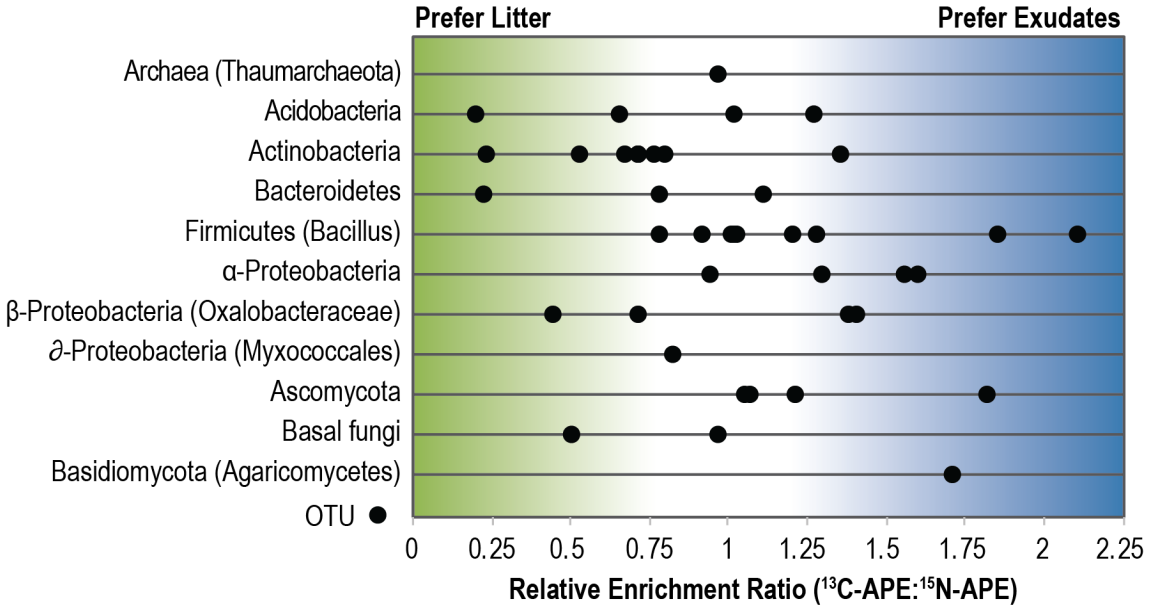


**Figure 5.** Relative substrate preferences for Bacteria, Archaea, and Fungi detected by Chip-SIP. Each dot represents a taxon that was significantly enriched in $^{13}C$ or $^{15}N$ derived from $^{13}C$-exudates or $^{15}N$-root detritus. The x-axis is the ratio of the atom percent excess (APE) $^{13}C$ enrichment and $^{15}N$ enrichment for the probe set, which is a unitless relative measure; the ratio was corrected by 1.7 to account for dilution of the C signal by the chip surface. The position of the taxon along the x-axis indicates its preference for exudates or root litter. Those that are positioned towards the left (green) incorporated relatively more isotope from $^{15}N$-litter whereas those that are positioned towards the right (blue) incorporated relatively more isotope from $^{13}C$-exudates. Probes targeting protists and nematodes were on the chip (Table S1) but we did not measure any significant enrichment in this 3-day $^{13}CO_2$ experiment.

# SUPPLEMENTAL

## Production of $^{15}$N-labeled root litter

To create $^{15}$N-labeled root litter, *Avena fatua* was grown for 8 weeks in fritted clay and fertilized solely with a custom mixture of Hoagland's plant nutrient solution, where the nitrogen-containing compounds were replaced with their 99 atom % $^{15}$N analogs (0.505 g/L $K^{15}NO_3$ (Cambridge Isotope Laboratories), 0.59 g/L $Ca(^{15}NO_3)_2 \times 4H_2O$ (Cambridge Isotope Laboratories), 0.0225 g/L Sprint 330 iron chelate (Becker Underwood), 0.493 g/L $MgSO_4 \times 7H_2O$, 0.080 g/L $^{15}NH_4{}^{15}NO_3$ (Cambridge Isotope Laboratories), 2.86 g/L $H_3BO_3$, 1.81 g/L $MnCl_2 \times 4H_2O$, 0.22 g/L $ZnSO_4 \times 7H_2O$, 0.051 g/L $CuSO_4$, 0.09 g/L $H_3MoO_4 \times H_2O$, and 0.5 ml/L of 1M $KH_2PO_4$ (pH 6.0)). Roots were triple washed in deionized water, dried, and stored for 1 year prior to use. Roots were chopped to ca. 1 mm lengths using scissors.

## Data processing using EMIRGE

Since EMIRGE probabilistically reconstructs sequences, the near full-length sequences have a higher error rate than sequences directly generated by Illumina sequencing. To address this, singletons and sequences present in only one sample were removed from the dataset. Next, we assessed the efficacy of three chimera checking tools to identify potential chimeras created by EMIRGE (UCHIME (62), DECIPHER (90), Chimera Slayer (91)), and determined that UCHIME was the most effective chimera-checking tool for our dataset. To assess the chimera-checking tools, we used a set of EMIRGE sequences reconstructed from a mock community composed of 52 known isolates available as a supplemental dataset from Miller, Baker (36). Any novel sequences in this EMIRGE dataset are likely chimeras, since the SSU sequences of all the community members are known. We determined that 3 of 23 reconstructed sequences were

548 putative chimeras, since they were < 90% similar to organisms in the NCBI database using
549 BLAST. We tested each chimera-detection method to determine if it could identify these 3
550 sequences in the EMIRGE dataset. Only UCHIME was capable of detecting chimeras in the
551 dataset; it was able to identify 2 of the 3 putative chimeras. Therefore, UCHIME was used for
552 chimera-checking analyses.
553
554 **Probe design:** We designed a custom Chip-SIP array for rhizosphere soil with probes targeting
555 bacteria, archaea, and eukaryotes (fungi, protists, nematodes). Probes were designed from the
556 sequences reconstructed by EMIRGE from the four treatments in this experiment. The 180 most
557 abundant OTU from bacteria, archaea, and eukarya were targeted for probe design. The
558 microarray probes were designed in ARB using the following restrictions: (≤ 2 mismatches
559 tolerated, GC content < 80%, homopolymer runs ≤ 4bp) (65). Twenty-five different probes were
560 selected for each sequence that were unique relative to the SILVA database and RNA-Seq
561 databases. Based on preliminary fluorescence data (using soils from actual experiment), from
562 these 25 probes, we selected the 10 probes that had the highest hybridization scores to synthesize
563 on the final microarray (signal:noise ≥ 1.3). Sequences that had few probes with positive
564 fluorescence (signal:noise < 1.3) were added to the microarray by keeping 10 probes with the
565 best ARB score (a measure of how specific the probe is to the sequence of interest).
566
567 **Chip-SIP microarray synthesis:** Microarrays were coated with a conductive surface prior to
568 probe synthesis to eliminate charging during SIMS analysis. Glass slides coated with indium-tin
569 oxide (Sigma) were treated with an alkyl phosphonate hydroxy-linker to provide a starting
570 substrate for probe synthesis (92). Microarray probes (spot size = 17 μm) were synthesized using

a photolabile deprotection strategy (93) on a Nimblegen Maskless Array Synthesizer (Roche). The probe sets were laid out in horizontal lines across the chip. All the probes were printed three times in three replicate blocks on the microarray. Nimblegen synthesis reagents (Roche) were delivered through the Expedite system (PerSeptive Biosystems).

**Microarray hybridization:** Two microarrays are necessary for Chip-SIP: a standard fluorescence microarray and a separate NanoSIMS microarray. Fluorescence analysis is necessary to confirm that the probes are hybridized with RNA. However, labeling RNA with a fluorophore introduces $^{12}$C-carbon that dilutes the $^{13}$C signal. Therefore, the RNA samples were split for fluorescence and NanoSIMS analyses and the RNA used in the NanoSIMS analysis was left unlabeled. Microarrays were not replicated.

For fluorescence analysis, the RNA was labeled with Alexafluor 532 dye using the Ulysis kit (Invitrogen), and were incubated for 10 min at 90°C (2 µL RNA, 10 µL labeling buffer, 2 µL Alexafluor reagent) and subsequently fragmented. RNA for NanoSIMS analysis was not labeled, and instead preceded directly to fragmentation. Samples were fragmented using 5X fragmentation buffer (Affymetrix) for 10 min at 90°C. Fragmented RNA was purified using a Spin-OUT™ minicolumn (Millipore), and RNA was concentrated by ethanol precipitation to a final concentration of 500 ng $\mu L^{-1}$. For array hybridization, RNA samples were mixed with 1X Hybridization buffer (Nimblegen) and placed in a Nimblegen X4 mixer slide. The arrays were incubated inside a Maui hybridization system (BioMicro Systems) for 18 hrs at 42°C and then washed according to manufacturer's instructions (Nimblegen).

Arrays with fluorescently labeled RNA were imaged with a Genepix 4000B fluorescence scanner at pmt = 650 units. Arrays with non-fluorescently labeled RNA were marked with a diamond pen and also imaged with the fluorescence scanner to subsequently navigate to the analysis spots in the NanoSIMS. Slides were trimmed and mounted in custom-built stainless-steel holders.

**Chip-SIP NanoSIMS analyses:** Mass resolution was set to ~10,000 mass resolving power to minimize the contribution of isobaric interferences to the species of interest (e.g., so that $^{11}B^{16}O^-$ contributes < 1/100 of the $^{13}C^{14}N^-$ ratio, and $^{13}C_2^-$ contributes < 1/1000 of the $^{12}C^{14}N^-$ ratio). Analyses were performed in imaging mode to generate digital ion images of the microarray for each ion species. The primary beam current was 5 to 7 pA $Cs^+$, which yielded a spatial resolution of 200-400 nm and a maximum count rate on the detectors of ~300,000 cps $^{12}C^{14}N$. Analysis area was 50 x 50 $\mu m^2$ with a pixel density of 256 x 256 with 0.5 or 1 ms/pixel dwell time. Ion counts were corrected for detector dead time on a pixel-by-pixel basis.

**Chip-SIP statistical analyses:** Individual 50 x 50 $\mu m^2$ isotope ratio images were stitched together to create an isotope map of the microarray surface using custom software developed for NanoSIMS analysis (L'image, L. Nittler, Carnegie Institution of Washington). Probe spot regions of interest (ROIs) were selected by hand or with an autodefinition function, and $^{15}N/^{14}N$ and $^{13}C/^{12}C$ isotope ratios were calculated for each ROI. Isotope ratios were converted to atom percent excess (APE) values using the formula $APE = [R_{meas}/(1 + R_{meas}) - R_{control}/(1 + R_{control})] \times 100\%$, where $R_{meas}$ is the isotope ratio measured by NanoSIMS and $R_{control}$ is the mean $^{15}N$ APE or $^{13}C$ APE value for the control probe locations. The presence of RNA on each probe was

616 confirmed using a separate fluorescence microarray analysis, where hybridized probes had a
617 signal to noise ratio > 1.3.
618
619 Two criteria identified which OTUs were enriched with $^{13}C$ or $^{15}N$. First, each probe set was
620 required to have five of ten probes with a signal:noise ratio > 1.3; this determined which OTUs
621 were present in the dataset. Second, each probe set had to have five probes with enrichment of
622 either >0.020 $^{13}C$ atom percent excess (APE) or >0.011 $^{15}N$ APE (equivalent to 30‰ for both).
623 For the OTUs that met these criteria, we calculated a $^{13}C$-APE:$^{15}N$-APE ratio for the entire probe
624 set by averaging all APE enrichments > 0 for $^{13}C$ and $^{15}N$ and then dividing the two averages
625 (average $^{13}C$ APE / average $^{15}N$ APE).
626
627

A. $^{15}$N APE B. $^{13}$C APE

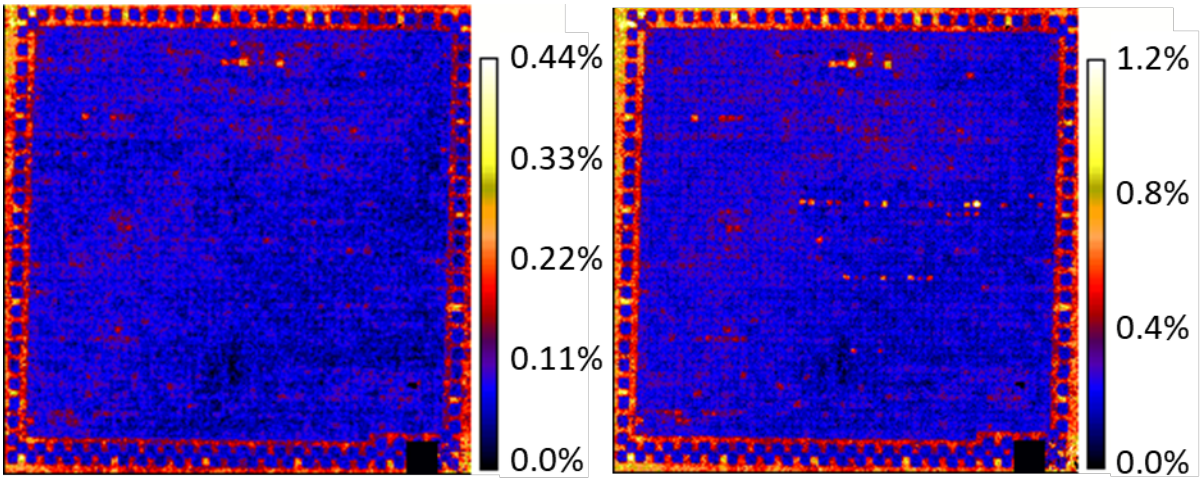


**Figure S1.** Chip-SIP isotope maps of a single phylogenetic microarray hybridized with isotopically labeled RNA from a rhizosphere soil microbial community exposed to $^{15}$N-labeled root detritus and $^{13}$C-exudates. As the microbes consume the substrates with the different isotope labels, they assimilate the isotopes into their microbial biomass and nucleic acids, and their preference for the $^{15}$N-root litter or $^{13}$C-exudates is determined by the amount of (A) $^{15}$N and (B) $^{13}$C contained in the RNA hybridized to a probe set specific to each taxon. Color scale bars indicate atom percent excess (APE) enrichment of the microarray surface. Probes sets are arranged in horizontal lines on the chip. The brightest $^{13}$C-enriched probe sets with no visible corresponding $^{15}$N-enriched probes are from plant host RNA.

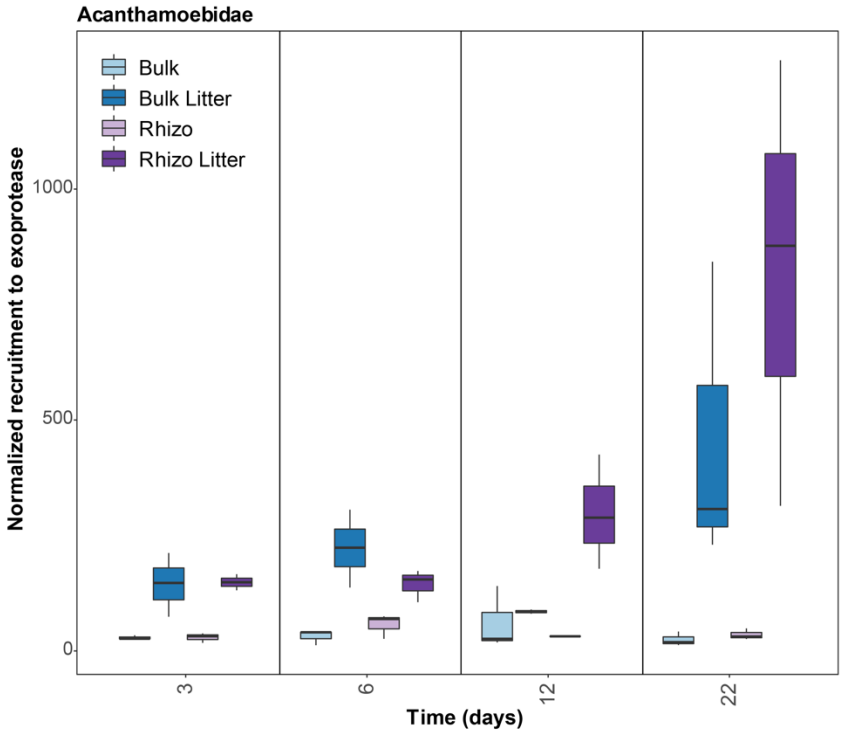


640

641 **Figure S2.** Acanthamoebidae exoprotease gene expression from a complimentary transcriptomic

642 dataset on the same soil (52) from 3-22 days. Rhizosphere and bulk soil were amended with

643 detrital root litter (Rhizo Litter, Bulk Litter) or unamended (Rhizo, Bulk). Sequences were

644 normalized using DESeq2 as previously (52).

645

646

## REFERENCES

1. Swift MJ, Anderson JM, Heal OW. Decomposition in terrestrial ecosystems. Oxford: Blackwell Publishing; 1979 Jan 1.

2. Scholes MC, Powlson D, Tian G. Input control of organic matter dynamics. *Geoderma* 1997; **79**: 25-47.

3. Greyston SJ, Vaughan D, Jones D. Rhizosphere carbon flow in trees, in comparison with annual plants: the importance of root exudation and its impact on microbial activity and nutrient availability. *Applied Soil Ecology* 1996; **5**: 29-56.

4. Schimel DS. Terrestrial biogeochemical cycles: Global estimates with remote sensing. *Remote Sens Environ* 1995; **51**: 49-56.

5. Sokol NW, Kuebbing SE, Ayala EK, Bradford MA. Evidence for the primacy of living root inputs, not root or shoot litter, in forming soil organic carbon. *The New phytologist* 2019; **221**: 233-46.

6. Bardgett RD. The Biology of Soil: A Community Ecosystem Approach. Oxford: Oxford University Press; 2005.

7. Schimel JP, Schaeffer SM. Microbial control over carbon cycling in soil. *Front Microbiol* 2012; **3**: 1-11.

8. Geisen S, Mitchell EAD, Wilkinson DM, Adl S, Bonkowski M, Brown MW, et al. Soil protistology rebooted: 30 fundamental questions to start with. *Soil Biol Biochem* 2017; **111**: 94-103.

9. Sinsabaugh RL, Moorhead DL. Resource allocation to extracellular enzyme production: a model for nitrogen and phosphorus control of litter decomposition. *Soil Biol Biochem* 1994; **26**: 1305-11.

10. Purahong W, Wubet T, Lentendu G, Schloter M, Pecyna MJ, Kapturska D, et al. Life in leaf litter: novel insights into community dynamics of bacteria and fungi during litter decomposition. *Mol Ecol* 2016; **25**: 4059-74.

11. Osono T. Ecology of ligninolytic fungi associated with leaf litter decomposition. *Ecol Res* 2007; **22**: 955-74.

12. Hattenschwiler S, Tiunov AV, Scheu S. Biodiversity and litter decomposition in terrestrial ecosystems. *Annual Review Of Ecology Evolution And Systematics* 2005; **36**: 191-218.

13. Pugh G. Terrestrial Fungi. In: Dickenson C, Pugh G, editors. Biology of Plant Litter Decomposition. 2. London: Academic Press Inc.; 1974. p. 303-36.

14. Geisen S, Koller R, Hünninghaus M, Dumack K, Urich T, Bonkowski M. The soil food web revisited: Diverse and widespread mycophagous soil protists. *Soil Biol Biochem* 2016; **94**: 10-8.

15. Chakraborty S, Old K. Ultrastructure and description of a fungus-feeding amoeba, *Trichamoeba mycophaga* n. sp. (Amoebidae, Amoebea), from Australia. *J Eukaryot Microbiol* 1986; **33**: 564-9.

16. Bjørnlund L, Rønn R. 'David and Goliath'of the soil food web–Flagellates that kill nematodes. *Soil Biol Biochem* 2008; **40**: 2032-9.

17. Xiong W, Jousset A, Guo S, Karlsson I, Zhao Q, Wu H, et al. Soil protist communities form a dynamic hub in the soil microbiome. *ISME J* 2018; **12**: 634-8.

18. Neher DA, Weicht TR, Barbercheck ME. Linking invertebrate communities to decomposition rate and nitrogen availability in pine forest soils. *Appl Soil Ecol* 2012; **54**: 14-23.

691 19. Bokhorst S, Wardle DA. Microclimate within litter bags of different mesh size:
692 Implications for the 'arthropod effect' on litter decomposition. *Soil Biol Biochem* 2013; **58**: 147-
693 52.
694 20. Carrillo Y, Ball BA, Bradford MA, Jordan CF, Molina M. Soil fauna alter the effects of
695 litter composition on nitrogen cycling in a mineral soil. *Soil Biol Biochem* 2011; **43**: 1440-9.
696 21. Riutta T, Slade EM, Bebber DP, Taylor ME, Malhi Y, Riordan P, et al. Experimental
697 evidence for the interacting effects of forest edge, moisture and soil macrofauna on leaf litter
698 decomposition. *Soil Biol Biochem* 2012; **49**: 124-31.
699 22. Meyer WM, Ostertag R, Cowie RH. Macro-invertebrates accelerate litter decomposition
700 and nutrient release in a Hawaiian rainforest. *Soil Biol Biochem* 2011; **43**: 206-11.
701 23. Stout JD. The Relationship between Protozoan Populations and Biological Activity in
702 Soils. *Integr Comp Biol* 1973; **13**: 193-201.
703 24. Bonkowski M, Griffiths B, Scrimgeour C. Substrate heterogeneity and microfauna in soil
704 organic 'hotspots' as determinants of nitrogen capture and growth of ryegrass. *Appl Soil Ecol*
705 2000; **14**: 37-53.
706 25. Tedersoo L, Anslan S. Towards PacBio-based pan-eukaryote metabarcoding using full-
707 length ITS sequences. *Environmental Microbiology Reports* 2019; **11**: 659-68.
708 26. Tedersoo L, Anslan S, Bahram M, Põlme S, Riit T, Liiv I, et al. Shotgun metagenomes
709 and multiple primer pair-barcode combinations of amplicons reveal biases in metabarcoding
710 analyses of fungi. *Mycokeys* 2015; **10**: 1-43.
711 27. Guillou L, Bachar D, Audic S, Bass D, Berney C, Bittner L, et al. The Protist Ribosomal
712 Reference database (PR2): a catalog of unicellular eukaryote Small Sub-Unit rRNA sequences
713 with curated taxonomy. *Nucleic Acids Res* 2013; **41**: D597-D604.

714 28. Baldrian P, Kolařík M, Štursová M, Kopecký J, Valášková V, Větrovský T, et al. Active
715 and total microbial communities in forest soil are largely different and highly stratified during
716 decomposition. *ISME J* 2012; **6**: 248-58.
717 29. Poisot T, Péquin B, Gravel D. High-Throughput Sequencing: A Roadmap Toward
718 Community Ecology. *Ecology and Evolution* 2013; **3**: 1125-39.
719 30. Nguyen NH, Smith D, Peay K, Kennedy P. Parsing ecological signal from noise in next
720 generation amplicon sequencing. *New Phytol* 2015; **205**: 1389-93.
721 31. Engelbrektson A, Kunin V, Wrighton KC, Zvenigorodsky N, Chen F, Ochman H, et al.
722 Experimental factors affecting PCR-based estimates of microbial species richness and evenness.
723 *ISME J* 2010; **4**: 642-7.
724 32. Suzuki MT, Giovannoni SJ. Bias caused by template annealing in the amplification of
725 mixtures of 16S rRNA genes by PCR. *Appl Environ Microbiol* 1996; **62**: 625-30.
726 33. Soergel D, Dey N, Knight R, Brenner S. Selection of primers for optimal taxonomic
727 classification of environmental 16S rRNA gene sequences. *ISME J* 2012; **6**: 1440-4.
728 34. Nomura M, Gourse R, Baughman G. Regulation of the synthesis of ribosomes and
729 ribosomal components. *Annu Rev Biochem* 1984; **53**: 75-117.
730 35. Urich T, Lanzén A, Qi J, Huson DH, Schleper C, Schuster SC. Simultaneous assessment
731 of soil microbial community structure and function through analysis of the meta-transcriptome.
732 *PLoS ONE* 2008; **3**: e2527.
733 36. Miller CS, Baker BJ, Thomas BC, Singer SW, Banfield JF. EMIRGE: reconstruction of
734 full-length ribosomal genes from microbial community short read sequencing data. *Genome*
735 *biology* 2011; **12**: R44.

736 37. Xue Y, Lanzén A, Jonassen I. Reconstructing ribosomal genes from large scale total
737 RNA meta-transcriptomic data. *Bioinformatics* 2020; **36**: 3365-71.
738 38. Bang-Andreasen T, Anwar MZ, Lanzén A, Kjøller R, Rønn R, Ekelund F, et al. Total
739 RNA-sequencing reveals multi-level microbial community changes and functional responses to
740 wood ash application in agricultural and forest soil. *FEMS Microbiol Ecol* 2020; **96**.
741 39. Geisen S, Tveit AT, Clark IM, Richter A, Svenning MM, Bonkowski M, et al.
742 Metatranscriptomic census of active protists in soils. *ISME J* 2015; **9**: 2178-90.
743 40. Adl SM, Habura A, Eglit Y. Amplification primers of SSU rDNA for soil protists. *Soil*
744 *Biol Biochem* 2014; **69**: 328-42.
745 41. Wagner M, P. H. Nielsen, A. Loy, J. L. Nielsen, and H. Daims. Linking microbial
746 community structure with function: fluorescence in situ hybridization-microautoradiography and
747 isotope arrays. . *Curr Opin Biotechnol* 2006; **17**: 83-91.
748 42. Neufeld J, Wagner M, Murrell J. Who eats what, where and when? Isotope-labelling
749 experiments are coming of age. *ISME J* 2007; **1**: 103-10.
750 43. Radajewski S, Ineson P, Parekh NR, Murrell J. Stable-isotope probing as a tool in
751 microbial ecology. *Nature* 2000; **403**: 646-9.
752 44. Radajewski S, Murrell JC. Stable Isotope Probing for Detection of Methanotrophs After
753 Enrichment with 13CH4. In: de Muro MA, Rapley R, editors. Gene Probes: Principles and
754 Protocols. Totowa, NJ: Humana Press; 2002. p. 149-57.
755 45. Manefield M, Whiteley AS, Griffiths R, Bailey MJ. RNA Stable Isotope Probing, a
756 Novel Means of Linking Microbial Community Function to Phylogeny. *Appl Environ Microbiol*
757 2002.

758 46. Mayali X, Weber PK, Nuccio E, Lietard J, Somoza M, Blazewicz SJ, et al. Stable Isotope
759 Probing, Methods and Protocols. *Methods in Molecular Biology* 2019; **2046**: 71-87.
760 47. Mayali X, Weber PK, Brodie EL, Mabery S, Hoeprich PD, Pett-Ridge J. High-throughput
761 isotopic analysis of RNA microarrays to quantify microbial resource use. *ISME J* 2012; **6**: 1210-
762 21.
763 48. Waldrop MP, Firestone MK. Seasonal dynamics of microbial community composition
764 and function in oak canopy and open grassland soils. *Microb Ecol* 2006; **52**: 470-9.
765 49. Shi S, Nuccio E, Herman DJ, Rijkers R, Estera K, Li J, et al. Successional Trajectories of
766 Rhizosphere Bacterial Communities over Consecutive Seasons. *mBio* 2015; **6**: e00746.
767 50. DeAngelis KM, Brodie EL, DeSantis T, Andersen G, Lindow S, Firestone MK. Selective
768 progressive response of soil microbial community to wild oat. *ISME J* 2009; **3**: 168-78.
769 51. Jaeger CH, Lindow SE, Miller W, Clark E, Firestone MK. Mapping of sugar and amino
770 acid availability in soil around roots with bacterial sensors of sucrose and tryptophan. *Appl*
771 *Environ Microbiol* 1999; **65**: 2685-90.
772 52. Nuccio EE, Starr E, Karaoz U, Brodie EL, Zhou J, Tringe SG, et al. Niche differentiation
773 is spatially and temporally regulated in the rhizosphere. *ISME J* 2020; **269**: 1-16.
774 53. Griffiths RI, Whiteley AS, O'Donnell AG, Bailey M. Rapid method for coextraction of
775 DNA and RNA from natural environments for analysis of ribosomal DNA- and rRNA-based
776 microbial community composition. *Appl Environ Microbiol* 2000; **66**: 5488-91.
777 54. Andrews S. FastQC: A Quality Control tool for High Throughput Sequence Data
778 (Version 0.10.1) 2012; http://www.bioinformatics.babraham.ac.uk/projects/fastqc/
779 55. Bolger AM, Lohse M, Usadel B. Trimmomatic: a flexible trimmer for Illumina sequence
780 data. *Bioinformatics* 2014; **30**: 2114-20.

781 56. McDonald D, Price MN, Goodrich J, Nawrocki EP, DeSantis TZ, Probst A, et al. An
782 improved Greengenes taxonomy with explicit ranks for ecological and evolutionary analyses of
783 bacteria and archaea. *ISME J* 2012; **6**: 610-8.
784 57. Quast C, Pruesse E, Yilmaz P, Gerken J, Schweer T, Yarza P, et al. The SILVA
785 ribosomal RNA gene database project: improved data processing and web-based tools. *Nucleic*
786 *Acids Res* 2013; **41**: D590-D6.
787 58. Langmead B, Trapnell C, Pop M, Salzberg SL. Ultrafast and memory-efficient alignment
788 of short DNA sequences to the human genome. *Genome biology* 2009; **10**: R25.
789 59. Edgar RC. UPARSE: highly accurate OTU sequences from microbial amplicon reads.
790 *Nat Methods* 2013; **10**: 996 - 8.
791 60. Caporaso JG, Kuczynski J, Stombaugh J, Bittinger K, Bushman FD, Costello EK, et al.
792 QIIME allows analysis of high-throughput community sequencing data. *Nat Methods* 2010; **7**:
793 335-6.
794 61. Wang Q, Garrity GM, Tiedje JM, Cole JR. Naive Bayesian classifier for rapid
795 assignment of rRNA sequences into the new bacterial taxonomy. *Appl Environ Microbiol* 2007;
796 **73**: 5261-7.
797 62. Edgar RC, Haas BJ, Clemente JC, Quince C, Knight R. UCHIME improves sensitivity
798 and speed of chimera detection. *Bioinformatics* 2011; **27**: 2194-200.
799 63. Miller CS, Handley KM, Wrighton KC, Frischkorn KR, Thomas BC, Banfield JF. Short-
800 read assembly of full-length 16S amplicons reveals bacterial diversity in subsurface sediments.
801 *PLoS ONE* 2013; **8**: e56018.
802 64. Lozupone C, Knight R. UniFrac: a new phylogenetic method for comparing microbial
803 communities. *Appl Environ Microbiol* 2005; **71**: 8228-35.

804 65. Ludwig W, Strunk O, Westram R, Richter L, Meier H, Yadhukumar, et al. ARB: a
805 software environment for sequence data. *Nucleic Acids Res* 2004; **32**: 1363-71.
806 66. Mayali X, Weber PK, Pett-Ridge J. Taxon-specific C/N relative use efficiency for amino
807 acids in an estuarine community. *FEMS Microbiol Ecol* 2013; **83**: 402-12.
808 67. de Ruiter PC, Neutel AM, Moore JC. Energetics, patterns of interaction strengths, and
809 stability in real ecosystems. *Science* 1995; **269**: 1257-60.
810 68. Glücksman E, Bell T, Griffiths RI, Bass D. Closely related protist strains have different
811 grazing impacts on natural bacterial communities. *Environ Microbiol* 2010; **12**: 3105-13.
812 69. Yeates GW, Bongers T, De Goede R, Freckman DW, Georgieva SS. Feeding habits in
813 soil nematode families and genera—an outline for soil ecologists. *J Nematol* 1993; **25**: 315-31.
814 70. Griffiths BS. Microbial-feeding nematodes and protozoa in soil: Their effectson
815 microbial activity and nitrogen mineralization in decomposition hotspots and the rhizosphere.
816 *Plant Soil* 1994; **164**: 25-33.
817 71. Bonkowski M, Clarholm M. Stimulation of plant growth through interactions of bacteria
818 and protozoa: testing the auxiliary microbial loop hypothesis. *Acta Protozool* 2012; **51**: 237-47.
819 72. Clarholm M. Interactions of bacteria, protozoa and plants leading to mineralization of soil
820 nitrogen. *Soil Biol Biochem* 1985; **17**: 181-7.
821 73. Gao Z, Karlsson I, Geisen S, Kowalchuk G, Jousset A. Protists: Puppet Masters of the
822 Rhizosphere Microbiome. *Trends Plant Sci* 2019; **24**: 165-76.
823 74. Bates ST, Clemente JC, Flores GE, Walters WA, Parfrey LW, Knight R, et al. Global
824 biogeography of highly diverse protistan communities in soil. *ISME J* 2013; **7**: 652-9.
825 75. el Zahar Haichar F, Achouak W, Christen R. Identification of cellulolytic bacteria in soil
826 by stable isotope probing. *Environ Microbiol* 2007; **9**: 625-34.

827 76. Lee CG, Watanabe T, Sato Y, Murase J, Asakawa S, Kimura M. Bacterial populations
828 assimilating carbon from 13C-labeled plant residue in soil: Analysis by a DNA-SIP approach.
829 *Soil Biol Biochem* 2011; **43**: 814-22.
830 77. Eichorst SA, Kuske CR. Identification of cellulose-responsive bacterial and fungal
831 communities in geographically and edaphically different soils by using stable isotope probing.
832 *Appl Environ Microbiol* 2012; **78**: 2316-27.
833 78. Okada H, Harada H, Kadota I. Fungal-feeding habits of six nematode isolates in the
834 genus Filenchus. *Soil Biol Biochem* 2005; **37**: 1113-20.
835 79. Rotem O, Pasternak Z, Jurkevitch E. Bdellovibrio and Like Organisms. In: Rosenberg E,
836 DeLong EF, Lory S, Stackebrandt E, Thompson F, editors. The Prokaryotes, Deltaproteobacteria
837 and Epsilonproteobacteria. Berlin: Springer-Verlag; 2014. p. 3-17.
838 80. Leveau JHJ, Uroz S, Boer WD. The bacterial genus Collimonas: mycophagy, weathering
839 and other adaptive solutions to life in oligotrophic soil environments. *Environ Microbiol* 2010;
840 **12**: 281-92.
841 81. Cotrufo MF, Wallenstein MD, Boot CM, Denef K, Paul E. The Microbial Efficiency-
842 Matrix Stabilization (MEMS) framework integrates plant litter decomposition with soil organic
843 matter stabilization: do labile plant inputs form stable soil organic matter? *Global Change Biol*
844 2013; **19**: 988-95.
845 82. Wickings K, Grandy AS, Reed SC, Cleveland CC. The origin of litter chemical
846 complexity during decomposition. *Ecol Lett* 2012; **15**: 1180-8.
847 83. Schmidt MWI, Torn MS, Abiven S, Dittmar T, Guggenberger G, Janssens IA, et al.
848 Persistence of soil organic matter as an ecosystem property. *Nature* 2011; **478**: 49-56.

849 84. Allison SD, Martiny JB. Resistance, resilience, and redundancy in microbial
850 communities. *Proc Natl Acad Sci USA* 2008; **105**: 11512-9.
851 85. Sutton R, Sposito G. Molecular structure in soil humic substances: The new view.
852 *Environmental Science & Technology* 2005; **39**: 9009-15.
853 86. Kleber M, Sollins P, Sutton R. A conceptual model of organo-mineral interactions in
854 soils: self-assembly of organic molecular fragments into zonal structures on mineral surfaces.
855 *Biogeochemistry* 2007; **85**: 9-24.
856 87. Kögel-Knabner I. The macromolecular organic composition of plant and microbial
857 residues as inputs to soil organic matter. *Soil Biol Biochem* 2002; **34**: 139-62.
858 88. Amelung W, Brodowski S, Sandhage-Hofmann A, Bol R. Combining biomarker with
859 stable isotope analyses for assessing the transformation and turnover of soil organic matter.
860 *Advances in agronomy* 2008; **100**: 155-250.
861 89. Halter D, Goulhen-Chollet F, Gallien S, Casiot C, Hamelin J, Gilard F, et al. In situ
862 proteo-metabolomics reveals metabolite secretion by the acid mine drainage bio-indicator,
863 Euglena mutabilis. *ISME J* 2012; **6**: 1391-402.
864 90. Wright ES, Yilmaz LS, Noguera DR. DECIPHER, a search-based approach to chimera
865 identification for 16S rRNA sequences. *Appl Environ Microbiol* 2012; **78**: 717-25.
866 91. Haas BJ, Gevers D, Earl AM, Feldgarden M, Ward DV, Giannoukos G, et al. Chimeric
867 16S rRNA sequence formation and detection in Sanger and 454-pyrosequenced PCR amplicons.
868 *Genome Res* 2011; **21**: 494-504.
869 92. Pett-Ridge J, Hoeprich P, Weber P, Brodie E, inventors; Lawrence Livermore National
870 Security, assignee. Devices, Methods and Systems for Target Detection. USA2011.

871 93. Singh-Gasson S, Green RD, Yue Y, Nelson C, Blattner F, Sussman MR, et al. Maskless
872 fabrication of light-directed oligonucleotide microarrays using a digital micromirror array. *Nat*
873 *Biotechnol* 1999; **17**: 974-8.
874